

Externally Fed Accretion onto Protostars

Paul A. Dalba¹ and Steven W. Stahler¹

Sstahler@astro.berkeley.edu

ABSTRACT

The asymmetric molecular emission lines from dense cores reveal slow, inward motion in the clouds' outer regions. This motion is present both before and after the formation of a central star. Motivated by these observations, we revisit the classic problem of steady, spherical accretion of gas onto a gravitating point mass, but now include self-gravity of the gas and impose a finite, subsonic velocity as the outer boundary condition. We find that the accretion rate onto the protostar is lower than values obtained for isolated, collapsing clouds, by a factor that is the Mach number of the outer flow. Moreover, the region of infall surrounding the protostar spreads out more slowly, at a speed close to the subsonic, incoming velocity. Our calculation, while highly idealized, provides insight into two longstanding problems – the surprisingly low accretion luminosities of even the most deeply embedded stellar sources, and the failure so far to detect spatially extended, supersonic infall within their parent dense cores. Indeed, the observed subsonic contraction in the outer regions of dense cores following star formation appears to rule out a purely hydrodynamic origin for these clouds.

Subject headings: ISM: clouds, kinematics and dynamics — stars: formation — accretion

1. Introduction

Astronomers are elucidating, in much greater detail than ever before, the earliest phases of low-mass star formation. It has long been known that at least half of dense cores within molecular clouds do not yet contain young stars (Beichman et al. 1986). It is also known that these starless cores have, on average, less mass than cores with embedded stars (Jijina, Myers, & Adams 1999). What is now clearer is the chemical and structural progression of cores as they approach the collapse threshold and then cross it. The most centrally concentrated starless cores tend to exhibit the asymmetric emission line profiles signifying inward contraction, with the inferred velocity being several tenths of the sound speed (Lee, Myers, & Tafalla 2001). The same blueward asymmetry

¹Astronomy Department. University of California, Berkeley, CA 94720

is seen in those cores with embedded stars, where it is especially common (Mardones et al. 1997). Detailed examination of line profiles reveals no qualitative change across the collapse threshold, except for the appearance of broad wings that are attributable to molecular outflows (Gregersen et al. 2000).

It is likely that the contraction observed in starless cores is driven by self-gravity, as material in the core’s outer region settles toward the center (e.g., Ciolek & Basu 2001). A similar, exterior contraction should also occur in cores that have produced stars, and observations thus far support this conclusion. Here, targeted studies are rare, in part because outflows often contaminate the emission line spectra. As one example, Myers et al. (1996) utilized a simple radiative transfer model to measure the spatially averaged contraction speed in L1526, a core with an embedded star that drives a weak outflow. Their derived contraction speed of 0.025 km s^{-1} is indeed close to the inferred speeds in starless cores. The CS and H₂CO spectra for the low-mass infall candidates identified by Mardones et al. (1997) have a similar degree of asymmetry as L1526, but have not been modeled to this level of detail.

Taken as a whole, these observations suggest that a dense core reaches the point of collapse by accruing matter externally. The core itself is a relatively quiescent structure, since its observed emission lines have nearly thermal widths (Barranco & Goodman 1998). The exterior molecular gas, however, has typical speeds of 1 to 2 km s^{-1} , corresponding to Mach numbers of 5 to 10 (Bergin & Tafalla 2007). How exactly material passes from this environment into the core is unknown, despite increasingly detailed mapping of the transition region (Pineda et al. 2010). In any event, the core is dynamically evolving while it collects mass. Gas in its outer mantle creeps inward, and continues to do so even after the central region collapses to form a star.

The standard theory of collapse, first formulated prior to the discovery of dense cores, paints a very different picture. In the still widely used self-similar model of Shu (1977), the cloud is a perfectly static entity before the first appearance of a protostar. The impulsive suctioning of gas caused by this event sends out a sharp rarefaction wave, expanding at the speed of sound. It is within this wavefront that infall occurs. Gas leaves the rarefaction wave with zero velocity and attains the sound speed roughly halfway inside it.

For a typical dense core radius of 0.1 pc and sound speed of 0.2 km s^{-1} , the rarefaction wave reaches the boundary in 0.5 Myr. This interval, or one comparable, has been traditionally considered to be the lifetime of the protostar phase. Comparing the dynamical picture from theory with observations, it is striking that there are no known cores with embedded stars in which the sonic transition occurs reasonably close to the cloud boundary. On the contrary, the inferred location of this point in the best spectroscopic collapse candidates is only 0.01-0.02 pc from the protostar itself (Choi et al. 1995; Gregersen et al. 1997; Di Francesco et al. 2001; Belloche et al. 2002). Again, we must remember that strong molecular outflows can both mask and mimic large-scale motion in these studies. On the other hand, submillimeter continuum mapping of cores with embedded stars also indicates that infall is confined to a small, central region. Shirley, Evans, & Rawlings (2002)

have shown that more widespread collapse would give rise to a change in the interior density profile that is not observed. The continuing absence of dense cores that contain stars and exhibit true global infall is forcing us to conclude either that all observed protostars happen to be especially young, or else that infall actually spreads more slowly than traditional theory posits.

The collapse model of Shu (1977) also predicts that the mass accretion rate onto the protostar is a constant in time:

$$\dot{M} = m_{\circ} \frac{c_s^3}{G}. \quad (1)$$

Here, c_s is the isothermal sound speed in the core and m_{\circ} is a nondimensional number with a value of 0.975. Many authors, starting with Kenyon et al. (1990), have noted that the accretion luminosity associated with this rate exceeds those observed for embedded, infrared sources. Subsequent numerical simulations relaxed the assumption of self-similarity, but usually imposed a rigid boundary on the dense core, i.e., a fixed surface where the fluid velocity vanishes (e.g., Foster & Chevalier 1993; Ogino, Tomisaka, & Nakamura 1999; Vorobyov & Basu 2005). In these calculations, \dot{M} varies in time, but is even higher, at least before gas begins to drain from the boundary region. The sonic transition occurs only slightly inside this boundary (see Fig. 1 of Foster & Chevalier 1993).

In response to the persistent and growing disparity between theory and observation, researchers have taken two very different paths. Some have focused on the possibility that, while cloud collapse occurs in the traditional manner, infalling gas is retained in a circumstellar disk, and only released periodically in bursts onto the protostar (e.g., Dunham & Vorobyov 2012). If the duration of bursts is sufficiently brief, we could be viewing protostars only when \dot{M} is relatively low. Whatever the merits of this idea, it does not address the troubling aspects of collapse models generally. Protostellar luminosity and cloud collapse are clearly linked, and a solution that considers both is preferable.

Following this second, unified path, Fatuzzo, Adams, & Myers (2004) generalized the model of Shu (1977) and investigated the self-similar evolution of a cloud that has a specified velocity profile at the start. Gómez et al. (2007) and Gong & Ostriker (2009) simulated numerically the birth of a dense core as arising from the convergence of a supersonic inflow. Both groups tracked the evolution past the start of core collapse. Stahler & Yen (2009) used perturbation theory to find the contraction in starless cores that are just approaching collapse, and were able to reproduce the asymmetric emission lines (Stahler & Yen 2010).

In this brief contribution, we focus on how continuous, external mass addition to the dense core affects protostellar infall itself. We show that \dot{M} in this case is equal to c_s^3/G times a factor that is essentially the Mach number of the incoming flow. This key result is easy to understand physically. For a cloud that is marginally stable against self-gravity, the free-fall and sound-crossing times are comparable. It follows that the mean speed of infalling fluid elements in an isolated cloud undergoing collapse is approximately c_s . When accretion is imposed from the outside, this mean speed is closer to the externally impressed value. The mass transport rate is lowered by their ratio, which is the incoming Mach number.

Since the contraction speed in the outer portion of the dense core is well under c_s , the reduction in \dot{M} may be substantial. The accretion luminosity is similarly reduced from traditional values, alleviating the discrepancy between theory and observation in this regard. We further show that the region of infall spreads out at a speed that is close to the subsonic injection velocity in the core’s exterior. This relatively slow expansion helps to explain why global, supersonic infall has been difficult to observe.

In Section 2 below, we describe the physical problem to be solved, present the relevant equations in nondimensional form, and then give our method of solution. Section 3 presents numerical results. Finally, Section 4 compares our findings with those of other studies, and indicates future directions for extending this work.

2. Formulation of the Problem

2.1. Physical Assumptions

Dense cores are supported against self-gravity not only by thermal pressure, but also by the interstellar magnetic field, which penetrates their interior (Crutcher 1999). The limited data from polarization mapping indicate that the field has a relatively smooth spatial variation (Rao, Girart, & Marrone 2011), as would be expected from the absence of significant MHD wave motion. From a theoretical perspective, the objects are essentially magnetostatic structures. They must evolve quasi-statically, however, since at some point they undergo gravitational collapse. This evolution is facilitated both by ambipolar diffusion, i.e., the slippage of neutral gas across field lines, and by the addition of fresh material from the core’s surroundings.

There is no reason why the dense core’s accrual of gas should cease once that object has produced a central star. Prior to this event, the core had an extended period of slow evolution. Thus, the *internal* accretion rate onto the protostar has had ample time to adjust so as to match the *external* rate at which mass is continually added to the dense core. In other words, \dot{M} is determined by conditions far from the star itself. This was also the case in the traditional picture of an isolated cloud undergoing collapse, where \dot{M} is set by the global free-fall time. A new picture, more consistent with observations, is that a dense core harboring a stellar source is a temporary repository for material that drifts in from the environment on its way to the protostar.¹

To begin exploring the new picture qualitatively, we adopt a very simple model. We ignore magnetic forces entirely, and treat the dense core as a region of steady, isothermal flow surrounding the protostar. Recent observations by the Herschel satellite have shown vividly how dense cores

¹The near equality of internal and external accretion rates does *not* hold if the external gas is injected supersonically. In that case, simulations find that the inner rate undergoes a sharp, transient burst just after star formation, before ultimately equilibrating to the outer rate (see Fig. 13 of Gong & Ostriker 2009).

are nested inside pc-scale filaments (Men’shchikov et al. 2010). Hence, the inward flow of gas is assuredly anisotropic. We ignore this complication as well, and assume spherical symmetry. Every fluid element experiences both the gravitational force from the protostar and that from interior cloud gas. Our problem is thus identical to the classic inflow calculation of Bondi (1952), except that we include self-gravity of the gas.

Like Bondi, we apply the inner boundary condition that this material is in free fall onto the star. However, we no longer demand that the density approach a fixed value at spatial infinity (as did Chia 1978). Instead, we require that the *velocity* reach some imposed, subsonic value. Note again the critical difference from the many numerical collapse simulations, where the infall velocity was set to zero at some radius, effectively isolating the dense core from its surroundings. In effect, our imposition of a finite, bounding velocity means that we are treating protostellar accretion as a flow problem, rather than a collapse, which would necessitate a time-dependent treatment (see the discussion in Wandel 1984).

In reality, of course, the subsonic flow begins at a finite boundary. By taking this boundary to infinity, we are focusing, again for simplicity, on the earliest phase of protostellar accretion, when the mass of the central object is much less than that of the parent dense core.² Since observations indicate that the *final* protostar mass is no more than 20 to 30 percent that of the core (Alves, Lombardi, & Lada 2007; Rathborne et al. 2009), this early epoch spans a substantial fraction of the protostar’s total lifetime.

2.2. Quasi-Steady Flow

In spherical symmetry, momentum conservation in an isothermal, steady-state flow reads

$$u \frac{du}{dr} = -\frac{G(M_* + M_r)}{r^2} - \frac{c_s^2}{\rho} \frac{d\rho}{dr}. \quad (2)$$

Here, u is the fluid velocity, taken to be positive for inward motion. The quantities M_* and M_r are, respectively, the mass of the central protostar and that of the cloud gas interior to radius r . Finally, ρ is the mass density of the gas and c_s the isothermal sound speed. The cloud mass M_r and density ρ are related through

$$\frac{dM_r}{dr} = 4\pi r^2 \rho. \quad (3)$$

Since the flow is steady, the same mass per unit time crosses every spherical shell. Denoting this mass transport rate by \dot{M} , we have

$$\dot{M} = 4\pi r^2 \rho u. \quad (4)$$

²Specifically, we are requiring that $M_* \ll r_b c_s^2/G$, where r_b is the dense core boundary. The dense core itself is marginally unstable gravitationally, so the righthand side of this inequality is close to the core mass.

The inner boundary condition is that the velocity approach free fall onto the star:

$$\lim_{r \rightarrow 0} u = \sqrt{\frac{2GM_*}{r}} . \quad (5)$$

Equivalently, M_r must approach zero in this limit. We set our outer boundary condition at spatial infinity and demand that

$$\lim_{r \rightarrow \infty} u(r) = u_\infty , \quad (6)$$

where u_∞ is some fixed, subsonic velocity that is consistent with the spectroscopic observations.

Equation (4) incorporates our assumption that the inner accretion rate onto the star matches the outer rate imposed externally. In more detail, the match will not be exact, and the difference drives secular changes in the gas density and total core mass that only a full evolutionary calculation can track. Within the infall region, the assumption of steady state is justified as long as the crossing time through that region is brief compared to the time for M_* to increase significantly. After completing the calculation, we will verify its self-consistency in this regard in Section 4 below.

2.3. Nondimensionalization and Method of Solution

It is convenient to recast our dynamical equations into nondimensional form. We adopt, as basic quantities, G , M_* , and c_s . The solution is then characterized by a dimensionless parameter, the Mach number associated with the inflow at the boundary:

$$\beta \equiv u_\infty / c_s . \quad (7)$$

We define a nondimensional velocity as $\tilde{u} \equiv u/c_s$, and a nondimensional cloud mass as $\tilde{M}_r \equiv M_r/M_*$. In addition, we define a fiducial radius, density, and mass transport rate, respectively, as

$$r_o \equiv \frac{GM_*}{c_s^2} , \quad (8)$$

$$\rho_o \equiv \frac{c_s^6}{G^3 M_*^2} , \quad (9)$$

$$\dot{M}_o \equiv \frac{c_s^3}{G} , \quad (10)$$

and set $\tilde{r} \equiv r/r_o$ and $\tilde{\rho} \equiv \rho/\rho_o$.

Our dynamical equations become

$$\tilde{u} \frac{d\tilde{u}}{d\tilde{r}} = -\frac{1 + \tilde{M}_r}{\tilde{r}^2} - \frac{1}{\tilde{\rho}} \frac{d\tilde{\rho}}{d\tilde{r}} , \quad (11)$$

$$\frac{d\tilde{M}_r}{d\tilde{r}} = 4\pi \tilde{r}^2 \tilde{\rho} , \quad (12)$$

$$\lambda = 4\pi \tilde{r}^2 \tilde{\rho} \tilde{u} , \quad (13)$$

where $\lambda \equiv \dot{M}/\dot{M}_o$. The boundary conditions are

$$\lim_{\tilde{r} \rightarrow 0} \tilde{u} = \sqrt{\frac{2}{\tilde{r}}}, \quad (14)$$

$$\lim_{\tilde{r} \rightarrow \infty} \tilde{u} = \beta. \quad (15)$$

From now on, we drop all tildes and alert the reader whenever we revert to dimensional variables.

To solve this system, we first combine equations (12) and (13) into

$$\frac{dM_r}{dr} = \frac{\lambda}{u}. \quad (16)$$

Next, we take the logarithmic derivative of equation (13) and use the result to eliminate the density gradient in equation (11):

$$\left(u - \frac{1}{u}\right) \frac{du}{dr} = -\frac{1 + M_r}{r^2} + \frac{2}{r}. \quad (17)$$

The basic strategy is to solve equations (16) and (17) to obtain $u(r)$ and $M_r(r)$. Equation (13) then provides an algebraic relation for $\rho(r)$.

Before describing the solution technique in more detail, we first derive a simple relation between λ and β . First note that equation (16) tells us that dM_r/dr asymptotes to a finite value for large r . Thus, M_r itself increases without limit. On the other hand, since u approaches a finite value, du/dr must vanish asymptotically. The entire lefthand side of equation (17) thus also goes to zero. The vanishing of the righthand side of this equation leads us to conclude that

$$\lim_{r \rightarrow \infty} M_r = 2r, \quad (18)$$

confirming our previous claim that M_r increases indefinitely.

Equation (18) implies that

$$\lim_{r \rightarrow \infty} \frac{dM_r}{dr} = 2. \quad (19)$$

We now apply this same, large- r limit to equation (16). After utilizing equation (15), we find the desired relation:

$$\lambda = 2\beta. \quad (20)$$

In dimensional language, this is

$$\dot{M} = \left(\frac{2u_\infty}{c_s}\right) \frac{c_s^3}{G}. \quad (21)$$

Here we see explicitly the reduction factor modifying the conventional mass accretion rate.

Supplied with this result, we proceed to solve the coupled equations (16) and (17) as follows. We start at an r -value inside the sonic point r_s , i.e., the radius where $u = 1$. At this interior point r_i , we guess both u and M_r . Integrating outward, we find that $u(r)$ diverges upward or downward as we approach r_s , depending on the guessed $u(r_i)$. Using a bifurcation technique, we find that value

of $u(r_i)$ which extends the solution farthest out. We then integrate inward from r_i , and similarly find that the velocity either climbs above or falls below the free-fall value given by equation (14). A similar bifurcation technique then yields the best-fit M_r at $r = r_i$.

Having satisfied the inner boundary condition and established the location of the sonic point r_s , our next task is to cross this point. We apply L'Hôpital's rule to equation (17) and use equation (16) to find

$$\frac{du}{dr} = -\frac{\sqrt{1 - \lambda/2}}{r}, \quad \text{at } r = r_s. \quad (22)$$

This relation, together with the numerically established $M_r(r_s)$, allows us to integrate outward. As long as λ obeys equation (20), the velocity u automatically approaches β at large r .

3. Numerical Results

Figure 1 displays the velocity profile $u(r)$ obtained in the manner indicated. Here we have set the incoming Mach number equal to the representative value $\beta = 0.2$. Close to the origin, the velocity diverges as gas freely falls onto the protostar. Farther out, u first dips below β and then asymptotically approaches it through a series of decaying oscillations.

The sonic point is found to be $r_s = 0.544$, a slight increase over the Bondi value of 0.5. The *dimensional* sonic radius is then

$$r_s = \lambda \tilde{r}_s c_s t \quad (23a)$$

$$= 2 \tilde{r}_s \beta c_s t. \quad (23b)$$

Thus, the point moves out with speed

$$\frac{dr_s}{dt} = 2 \tilde{r}_s \beta c_s. \quad (24)$$

If we identify the infall region as that volume interior to r_s , then this region expands at $0.22 c_s$. Note again the contrast with the model of Shu (1977), where the equivalent speed is exactly c_s . Note also that the value of $2 \tilde{r}_s$ is close to unity and insensitive to β , rising only to 1.22 for $\beta = 0.4$. In summary, the infall region spreads out at a speed close to βc_s , at least during this early epoch.

Figure 2 shows the density profile $\rho(r)$. Inside r_s , the profile is that associated with freely falling gas. From equations (13), (14), and (20), this limiting profile is

$$\rho = \frac{\beta}{2\sqrt{2}\pi r^{3/2}} \quad r \ll r_s. \quad (25)$$

The dimensional equivalent is

$$\rho = \left(\frac{\beta}{c_s t}\right)^{1/2} \frac{c_s^2}{4\pi G r^{3/2}}, \quad (26)$$

where we have also used $M_* = \dot{M} t$. At early times, the density declines throughout the free-fall region, while the region itself expands.

Outside of r_s , equations (13), (15) and (20) tell us that

$$\rho = \frac{1}{2\pi r^2} \quad r \gg r_s . \quad (27)$$

which is dimensionally equivalent to

$$\rho = \frac{c_s^2}{2\pi G r^2} . \quad (28)$$

This is the profile of the singular isothermal sphere, as we expect for a self-gravitating gas cloud that contains a star of relatively small mass and is close to hydrostatic equilibrium (Stahler & Palla 2004, Chapter 9).

4. Discussion

Having solved the problem as posed, our next task is to check that the assumption of steady-state flow is reasonable. The outer portion of the cloud evolves slowly with time, as a structure that is never far from hydrostatic balance. It is the interior region that concerns us. Again, we need to make sure that the crossing time from r_s to the origin is less than M_*/\dot{M} , which in turn is close to the evolutionary time t .³ Thus, we require

$$\int_0^{r_s} \frac{dr}{u} < t . \quad (29)$$

But $u > c_s$ in this region, so that the integral is less than r_s/c_s . Since the infall region expands subsonically, this ratio is indeed less than t .

We stress the need for a fully time-dependent calculation to verify our main results. Assuming there is no qualitative change, it is instructive to compare our findings with those of Gong & Ostriker (2009). Using direct simulation, these authors built up a dense core from a spherically converging, supersonic flow. The accretion shock bounding the core first expands and then contracts supersonically before the core itself undergoes interior collapse. When the protostar first appears, the velocity profile throughout the dense core is uniform and supersonic, with $u \approx 3c_s$. A rarefaction wave erupts from the origin, but now expands supersonically. The wave quickly overtakes the accretion shock and effectively destroys it, so that the converging inflow thereafter directly impacts the protostar. Gong & Ostriker (2011) repeated the simulation using a planar, external flow and found substantially the same results.

³The time M_*/\dot{M} would *not* be close to t if \dot{M} varied rapidly in time, as it does in simulations of isolated, collapsing clouds. However, we do not expect such rapid variation when a subsonic, external flow is imposed from the start.

We observe once more the close relationship between the velocity of r_s and that of the gas introduced externally. To see this connection in yet another light, note that r_s is located roughly where the free-fall velocity onto the star matches the sound speed:

$$\sqrt{\frac{2GM_*}{r_s}} \approx c_s. \quad (30)$$

If we let $M_* = \dot{M} t$ and use equation (21), we find that $r_s \approx u_\infty t$.

The fact that the outer regions of dense cores are contracting subsonically *both before and after* the appearance of a protostar appears to rule out a purely hydrodynamic origin for these objects. The many researchers who have simulated cluster formation in turbulent molecular gas have effectively sidestepped this issue. In these studies, random velocity fluctuations are applied to a representative cube of molecular gas. Once these fluctuations thoroughly stir up the gas, self-gravity is switched on and overdense structures promptly collapse (see, e.g., Ballesteros-Paredes, Hartmann, & Vazquez-Semán 1999; Heitsch, Mac Low, & Klessen 2001; Padoan & Nordlund 2002; Offner, Klein, & McKee 2008).

More realistically, a dense core is self-gravitating and gains mass prior to this collapse, and a force in addition to the thermal pressure gradient must support it during this early epoch. This force is already known – the pressure gradient associated with the interstellar magnetic field. The field may not play a key role in the collapse phase studied here, although it apparently impacts the formation of circumstellar disks (Li, Krasnopolsky, & Shang 2011). In any case, the magnetic field is surely key in the early buildup of dense cores within their parent cloud filaments, and must also mediate the transition between the supersonic exterior of each core and its supersonic exterior.

We are grateful to Paola Caselli, Neal Evans, and Phil Myers for sharing their expertise on dense cores and the subtle ways in which observations are revealing their dynamics. SWS was partially supported by NSF Grant AST-0908573.

REFERENCES

- Alves, Lombardi, & Lada, 2007, *A&A*, 462, 17
- Ballesteros-Paredes, J., Hartmann, L., & Vazquez-Semadeni, E. *ApJ*, 527, 285
- Barranco, J. A. & Goodman, A. A. 1998, *ApJ*, 504, 207
- Beichman, C. A., Myers, P. C., Emerson, J. P., Harris, S., Mathieu, R., Benson, P. J., & Jennings, R. E. 1986, *ApJ*, 307, 337
- Belloche, A., André, P., Despois, D., & Blinder, S. 2002, *A&A*, 393, 927
- Bergin, E. A. & Tafalla, M. 2007, *ARA&A*, 45, 339
- Bondi, H. 1952, *MNRAS*, 112, 195
- Chia, T. T. 1978, *MNRAS*, 185, 561
- Choi, M., Evans, N. J., Gregersen, E. W., & Wang, Y. 1995, *ApJ*, 448, 742
- Ciolek, G. & Basu, S. 2001, *ApJ*, 547, 272
- Crutcher, R. M. 1999, *ApJ*, 520, 706
- Di Francesco, J., Myers, P. C., Wilner, D. J., Ohashi, N., & Mardones, D. 2001, *ApJ*, 562, 770
- Dunham, M. M. & Vorobyov, E. I. 2012, *ApJ*, 747, 52
- Fatuzzo, M. Adams, F. C., & Myers, P. C. 2002, *ApJ*, 615, 813
- Foster, P. N. & Chevalier, R. A. 1993, *ApJ*, 416, 30
- Gómez, G. C., Vázquez-Semadeni, E., Shadmehri, M., & Ballesteros-Paredes, J. 2007, *ApJ*, 669, 1042
- Gong, H. & Ostriker, E. C. 2009, *ApJ*, 699, 230
- Gong, H. & Ostriker, E. C. 2011, *ApJ*, 729, 120
- Gregersen, E. M., Evans, N. J., Zhou, S., & Choi, M. 1997, *ApJ*, 484, 256
- Gregersen, E. M., Evans, N. J., Mardones D., & Myers, P. C. 2000, *ApJ*, 533, 440
- Heitsch, F., Mac Low, M.-M., & Klessen, R. S. *ApJ*, 547, 280
- Jijina, J., Myers, P. C., & Adams, F. 1999, *ApJS*, 125, 161
- Kenyon, S. J., Hartmann, L. W., Strom, K. M., & Strom, S. E. 1990, *AJ*, 99, 869

- Lee, C. W., Myers, P. C., & Tafalla, M. 2001, *ApJS*, 136, 703
- Li, Z.-Y., Krasnopolsky, R., & Shang, H. 2011, *ApJ*, 738, 180
- Mardones, D., Myers, P. C., Tafalla, M., Wilner, D. J., Bachiller, R., & Garay, G. 1997, *ApJ*, 489, 719
- Men'shchikov, A. et al. 2010, *A&A*, 518, L103
- Myers, P. C., Evans, N. J., & Ohashi, N. 2000, in *Protostars and Planets IV*, ed. V. Mannings, A. P. Boss, & S. S. Russell, Tuscon: U. of Arizona, 21
- Myers, P. C., Mardones, D., Tafalla, M., Williams, J. P., & Wilner, D. J. 1996, *ApJ*, 465, L133
- Offner, S., Klein, R. I., & McKee, C. F. 2008, *ApJ*, 686, 1174
- Ogino, S., Tomisaka, K., & Nakamura, F. 1999, *PASJ*, 51, 637
- Padoan, P. & Nordlund, A. 2002, *ApJ*, 576, 870
- Pineda, J. E., Goodman, A. A., Arce, H. G., Caselli, P., Foster, J. B., Myers, P. C., & Rosolowsky, E. W. 2010, *ApJ*, 712, L116
- Rao, R., Girart, J.-M., & Marrone, D. P. 2011, in *Computational Star Formation: Proceedings of IAU Symposium No. 270*, eds. J. Alves, B. G. Elmegreen, J.-M. Girart, & V. Trimble, p. 103
- Rathborne, J. M., Lada, C. J., Muench, A. A., Alves, J. F., Kainulainen, J., & Lombardi, M., 2009, *ApJ*, 699, 742
- Shirley, Y. L., Evans, N. J., & Rawlings, J. M. C. 2002, *ApJ*, 575, 337
- Shu, F. H. 1977, *ApJ*, 214, 488
- Stahler, S. W. & Palla, F. 2004, *The Formation of Stars*, Wiley-VCH
- Stahler, S. W. & Yen, J. J. 2009, *MNRAS*, 396, 579
- Stahler, S. W. & Yen, J. J. 2011, *MNRAS*, 407, 2434
- Vorobyov, E. I. & Basu, S. 2005, *MNRAS*, 360, 675
- Wandel, A. 1984, *MNRAS*, 207, 861
- Zhou, S., Evans, N. J., Koempe, C., & Walmsley, C. M. 1993, *ApJ*, 404, 232

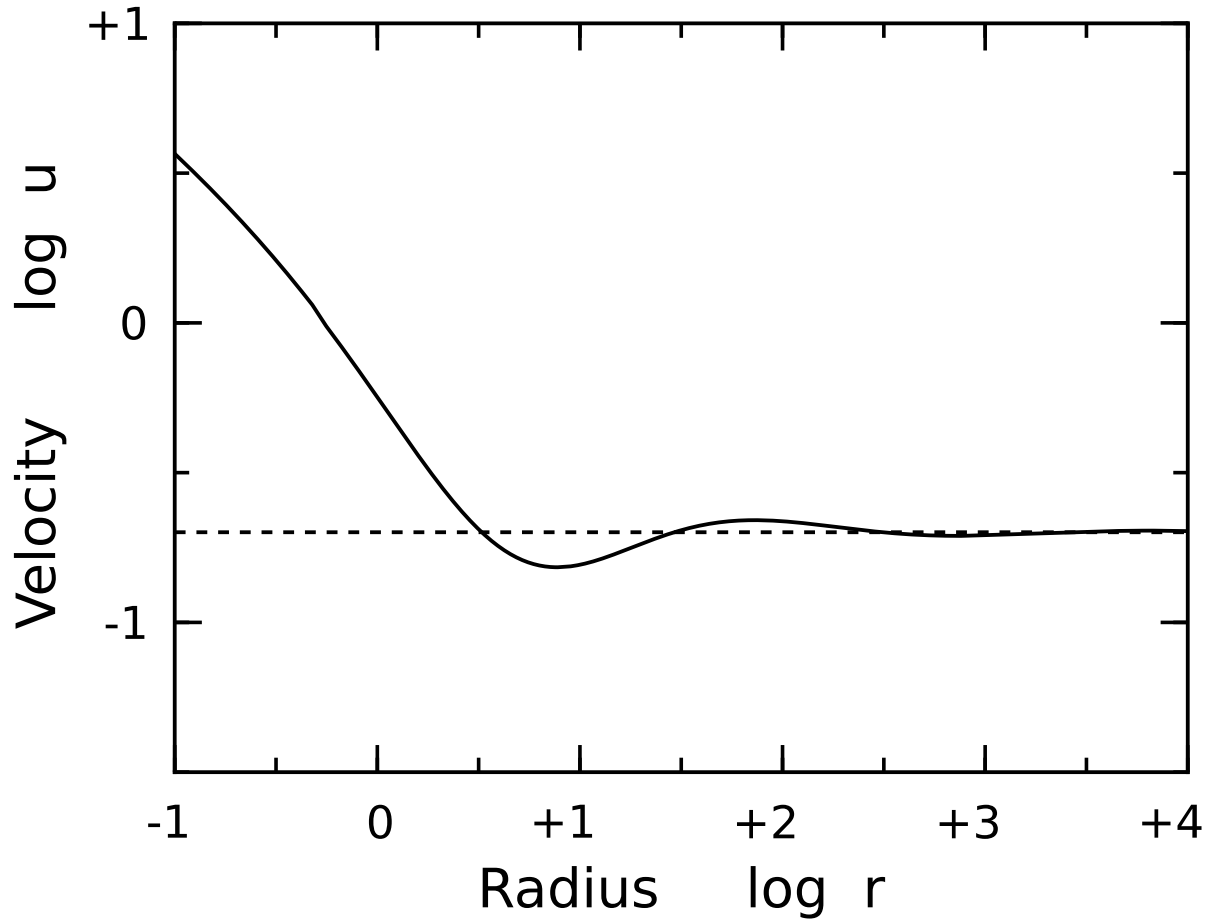


Fig. 1.— Velocity profile in the quasi-steady flow, for the representative case $\beta = 0.2$. Both the velocity and radius are in the nondimensional units defined in the text. The velocity asymptotically approaches the imposed, outer value, shown as the dashed, horizontal line.

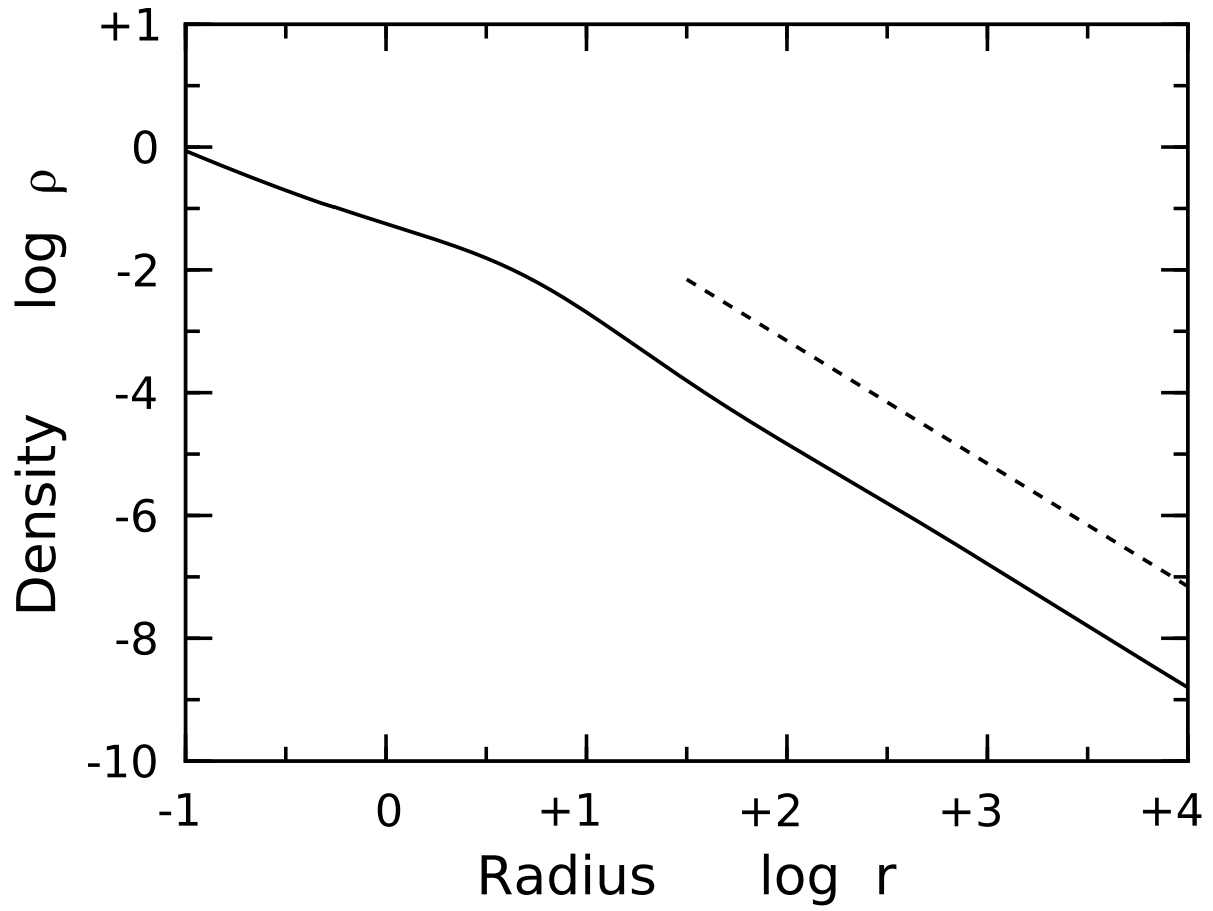


Fig. 2.— Density profile in the quasi-steady flow, for $\beta = 0.2$. The density and radius are both nondimensional. The dashed curve is a density profile that varies as r^{-2} .